

Technical report 07-002

# **Supervisory Hybrid Model Predictive Control for Voltage Stability of Power Networks\***

R. R. Negenborn, A. G. Beccuti, T. Demiray, S. Leirens, G. Damm,  
B. De Schutter, and M. Morari

*To cite this work, please refer to the published version:*

R. R. Negenborn, A. G. Beccuti, T. Demiray, S. Leirens, G. Damm, B. De Schutter, and M. Morari, "Supervisory hybrid model predictive control for voltage stability of power networks," *Proceedings of the 2007 American Control Conference*, New York, New York, pp. 5444–5449, July 2007. doi:[10.1109/ACC.2007.4282264](https://doi.org/10.1109/ACC.2007.4282264)

Delft Center for Systems and Control  
Delft University of Technology  
Mekelweg 2, 2628 CD Delft  
The Netherlands  
phone: +31-15-278.24.73 (secretary)  
URL: <https://www.dcsc.tudelft.nl>

---

\* This report can also be downloaded via <https://dpub.eu/07-002>

# Supervisory hybrid model predictive control for voltage stability of power networks

R.R. Negenborn, A.G. Beccuti, T. Demiray, S. Leirens, G. Damm, B. De Schutter, M. Morari

**Abstract**—Emergency voltage control problems in electric power networks have stimulated the interest for the implementation of online optimal control techniques. Briefly stated, voltage instability stems from the attempt of load dynamics to restore power consumption beyond the capability of the transmission and generation system. Typically, this situation occurs after the outage of one or more components in the network, such that the system cannot satisfy the load demand with the given inputs at a physically sustainable voltage profile. For a particular network, a supervisory control strategy based on model predictive control is proposed, which provides at discrete time steps inputs and set-points to lower-layer primary controllers based on the predicted behavior of a model featuring hybrid dynamics of the loads and the generation system.

## I. INTRODUCTION

Huge problems in the US and Canada [1], Italy, and The Netherlands due to power outages have shown the crucial role of a reliable operation of electricity distribution and transmission networks. A reliable and efficient operation of these networks is not only of paramount importance when these electricity systems are pressed to their limits of its performance, but also under regular operating conditions. Due to the deregulation in the European electricity market, the number and variety of actors increases. This number will even further increase as also large-scale industrial suppliers and small-scale individual households (via solar energy or wind energy installations) will start to feed electricity into the network [2]. With this increasing complexity faults and disturbances causing voltage instabilities are likely to occur more frequently.

In general, the behavior of power systems is characterized by complex interactions between continuous dynamics and discrete events, i.e., power systems exhibit hybrid behavior. Components such as generators and loads drive the continuous dynamic behavior. They obey physical laws, and are usually represented by coupled differential and algebraic equations. Discrete events or discrete inputs cause discrete behavior through, e.g., breaking down or connecting of a transmission line, saturation effects in automatic voltage regulators and power system stabilizers, *on* or *off* switching of

generators, connecting or disconnecting of loads, changing of transformer ratio settings, and connecting or disconnecting of capacitor banks; seasonal variations can also cause changes in power production capabilities as well as consumption and can modify the direction of power flows and thus cause switching behavior. The networks moreover typically span a wide range of time scales and large geographical areas.

To control such complex systems, hierarchical control in which control takes place at different layers based on space and/or time division is necessary [3]. The controllers at the lowest layer act directly on the actuators of the physical system, employing faster and more localized control. Higher-layer controllers supervise controllers of lower layers by providing set-points or specifying constraints, employing slower and more overall control. The task of a higher layer is to steer the underlying layer in such a way that the performance of the physical system is optimal in some sense. Traditionally in hierarchical control, a layer either only provides continuous or only discrete values to a different layer. In the approach we propose, both continuous and discrete values are dealt with in an integrated way, i.e., we consider a *hybrid* approach.

The particular control problem we are dealing with is voltage stability after disturbances. After a disturbance, e.g., breaking of a transmission line, the generation and transmission network may not have sufficient capacity to provide the loads with power; voltage instability may be the result. Control actions have to be chosen that minimize negative effects of this voltage instability. Traditionally, offline static stability studies are carried out in order to avert the occurrence of voltage instability. The approach we propose is an application of *online* control that takes into account both the inherent temporal dynamics and that determines the most appropriate control sequence required to reach an acceptable and secure operating point. We consider a scheme used by a higher-layer controller that controls a power network to determine both discrete and continuous set-points for lower-layer controllers in such a way that negative effects due to voltage instability after disturbances are minimized. We hereby assume that a lower layer that accepts set-points at discrete time steps is already present.

This paper is organized as follows. In Section II we introduce the power network and the lowest layer of control that we consider. In Section III we introduce the voltage control problem and the objectives. In Section IV we present a control strategy for the higher layer based on model predictive control. Section V contains simulation results obtained on the considered power network.

R.R. Negenborn and B. De Schutter are with the Delft Center for Systems and Control, Delft University of Technology, Delft, The Netherlands, r.r.negenborn@tudelft.nl, b@deschutter.info. A.G. Beccuti and M. Morari are with the Automatic Control Laboratory, ETH Zürich, Switzerland, {beccuti,morari}@control.ee.ethz.ch. T. Demiray is with the Power Systems Laboratory, ETH Zürich, Switzerland, demiray@eeh.ee.ethz.ch. S. Leirens is with the Automatic Control of Hybrid Systems group, Supélec, Rennes, France, sylvain.leirens@supelec.fr. G. Damm is with the Laboratoire Informatique, Biologie Intégrative et Systèmes Complexes, Université d'Evry-Val d'Essonne, Evry, France, Gilney.Damm@iup.univ-evry.fr.

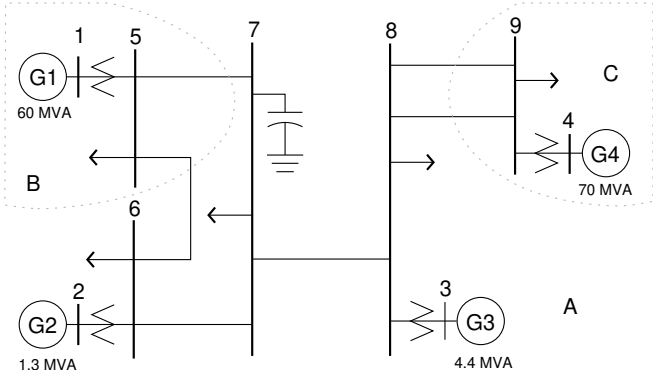


Fig. 1. Graphical representation of the IEEE 9-bus Anderson-Farmer network.

## II. POWER NETWORK SYSTEM

### A. Physical network

The case study under consideration is the 9 bus Anderson-Farmer network [4], depicted in Fig. 1, taken from the Dynamical Systems Benchmark Library<sup>1</sup>, whereto the reader is referred for an exhaustive description.

### B. Components of the network

The considered network consists of 4 generators  $G_1$ ,  $G_2$ ,  $G_3$  and  $G_4$  (shown with their nominal apparent power ratings) feeding the static loads at buses 5 through 9, where  $G_1$  and  $G_4$  and the loads connected to buses 5 and 9 are the aggregate representations for neighboring generators and loads. The synchronous machines are connected to the grid via lossless step-up transformers featuring a fixed turns ratio; a capacitor bank at node 7 provides additional reactive power to the system. The following list contains more details:

- **Generators:** Generators  $G_2$  and  $G_3$  represent single physical machines, whereas  $G_1$  and  $G_4$  denote the aggregate generators comprising several physical units. Therefore,  $G_2$  and  $G_3$  are described by a detailed sixth-order model [5] including the mechanical equations and the electrical transient and sub-transient dynamics, whereas  $G_1$  and  $G_4$  are described by second-order mechanical dynamics [5].
- **Loads:** The employed static loads comprise voltage dependent and constant impedance types [6]. The loads are described with following classical formulation in terms of active and reactive power

$$P_h = s_h P_{0h} v_h^\alpha \quad (1a)$$

$$Q_h = s_h Q_{0h} v_h^\alpha, \quad (1b)$$

where  $h \in \{5, 6, 7, 8, 9\}$ ,  $v_h$  is the voltage of bus  $h$ ,  $P_{0h}$  ( $Q_{0h}$ ) is the active (reactive) power steady-state value at node  $h$ , and  $s_h \in \{0, 0.02, \dots, 0.98, 1\}$  per unit (p.u.) represents the discrete load shedding factor applied to a load to relieve the strain of the power demand on the

system. Voltage dependent loads correspond to  $\alpha = 1$  and constant impedance loads to  $\alpha = 2$ .

- **Capacitor bank:** The capacitor bank locally stabilizes bus voltages by injecting additional reactive power into the grid. It is represented as a (negative) purely reactive load of type (1b) with  $\alpha = 2$  and thus describes a switched shunt capacitor.
- **Transmission lines:** The transmission lines between the buses and components transfer the power from one location to another. The lines are represented by the  $\pi$  model for transmission lines [5].

### C. Primary control layer

In the network there is a primary, lower-layer, control layer that locally regulates power flows and voltage levels at the bus terminals of generators. Fig. 2 shows a schematic representation of the local controllers' principle of operation. Feedback variables and corrective actions are depicted for each component [5]. The primary control layer consists of the following:

- **Turbine governors:** All generators feature a turbine governor (TG) controlling the mechanical power  $P_m$  acting on the shaft of the machine in order to satisfy the active power demand of the network and maintain the desired frequency  $\omega_{ref} = 60$  Hz. The TGs act on a time scale of tens of seconds.
- **Automatic voltage regulators:** All generators feature an automatic voltage regulator (AVR) maintaining the level of the excitation field  $E_{fd}$  in the rotor windings at the value required to keep the bus (stator) voltage close to the desired set-point. Saturation is included in the AVR to account for the maximum allowable current in the excitation system, i.e.,  $E_{fd}$  has an upper limit value  $E_{max}$  and a lower limit value  $E_{min}$ . Once a machine has reached its saturation limit it cannot produce additional reactive power and can therefore no longer participate in sustaining the voltages in the network [5]. The AVR voltage reference  $r_i$  of generator  $i$ ,  $i \in \{1, 2, 3, 4\}$ , can be set in the range  $0.9 - 1.1$  p.u. with steps of  $0.01$  p.u. The AVRs act on a time scale of seconds.

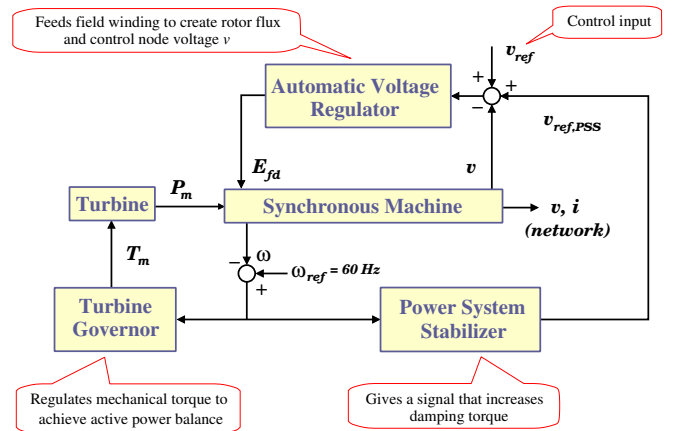


Fig. 2. Scheme of primary controllers at a generator.

<sup>1</sup>URL: <http://psdyn.ece.wisc.edu/IEEEbenchmarks/>

- Power system stabilizers: Generators  $G_2$  and  $G_3$  feature a power system stabilizer (PSS) eliminating the presence of unwanted rotor oscillations by measuring the rotational speed  $\omega$  and adding a corrective factor  $v_{\text{ref,PSS}}$  to the bus terminals' voltage reference  $v_{\text{ref}}$ . Generators  $G_1$  and  $G_4$  feature no power system stabilizer since the faster dynamics related to the rotor oscillations are not present in the related model equations. The PSSs act on a time scale of tenths of seconds.

#### D. Controls available to a higher control layer

Given the description of the network and the primary control layer, there is a number of controls available to a higher control layer in the form of set-point and reference settings. In particular the following can be adjusted:

- the voltage references for the AVRs;
- the mechanical power set-point for the TGs;
- the reference frequency for the TGs and PSSs;
- the amount of load to shed;
- the amount of capacitor banks to connect to the grid.

Depending on the particular control problem a higher-layer controller will adjust the values of these controls. In particular for the problem at hand the amount of load shed (defined by the variables  $s_h$ ) and the set-points of the AVRs (defined by the variables  $r_i$ ) will be taken as the available controls.

### III. EMERGENCY VOLTAGE CONTROL

A major source of power outages is voltage instability [7]. Voltage instability in general stems from the attempt of load dynamics to restore power consumption beyond the capability of the combined transmission and generation system. Typically, the capability is exceeded following the outage of one or more components in the network, such that the system cannot satisfy the load demand with the given inputs at a physically sustainable voltage profile in the network.

The control problem involves the case of emergency voltage regulation, in which the power system is initially in steady-state operation and subsequently subjected to a fault, modeled as the partial or total outage of a line. Due to the reduced transmission capacity of the network the requested load demand together with the given system configuration place the grid under an excessive amount of strain, so that corrective actions are required to avoid that the induced transients drive the system to collapse or cause unwanted and hazardous sustained oscillations. More specifically, the control objectives are:

- 1) Maintain the voltages between 0.9 and 1.1 p.u., i.e., sufficiently close to nominal values to ensure a safe operation of the system by keeping it sufficiently distant from low voltages, which may lead to a collapse.
- 2) Effectively achieve a steady-state point of operation, while minimizing switching of the control inputs so that a constant and appropriate set of input values is ultimately applied to the power grid.

For this second objective, in particular the option of shedding load is to be avoided unless absolutely necessary in order to

fulfill the primary objective, as load shedding is the most disruptive countermeasure available.

### IV. MODEL PREDICTIVE CONTROL

Model Predictive Control (MPC) [8], [9] has been traditionally employed in the process industry and has shown promising performance also for a variety of other control problems [10]. The control action is obtained at each time step by minimizing an objective function over a finite horizon subject to the equations of the employed prediction model and the operational constraints, e.g., on inputs. The control problem is solved in a receding horizon fashion. The major advantage of MPC is its straight-forward design procedure. Given a model of the system, hard constraints can be incorporated directly as inequalities and one only needs to set up an objective function reflecting the control aim; soft constraints can also be accounted for in the objective by using penalties for violations.

#### A. Derivation of the prediction model

The performance of a predictive controller relies for a large part on the accuracy of the prediction model of the system. The prediction model has to describe well how the inputs affect the system behavior. Ideally a perfect model of the system would be used; however, such a perfect model can be very complex, thus making the optimization procedure in the controller slow. Instead, an approximation is used. If this approximation fits in a suitable form, relatively efficient optimization techniques can be used to determine the controls (e.g., linear or mixed-integer linear programming).

In order for the higher-layer controller that we are designing to meet its control objectives, it has to be able to predict how set-point changes influence the dynamics of the network. Therefore, the controller uses a model that includes both a representation of the physical network and a representation of the primary control layer.

The network, including the primary control layer, is expressed [5] as a system of differential-algebraic equations (DAE)

$$\dot{x} = f(x, u, v) \quad (2a)$$

$$0 = g(x, u, v) \quad (2b)$$

where the state variables  $x$  are the generator dynamic variables,  $u$  denotes the system inputs, and the algebraic output variables  $v$  are the bus voltage magnitudes. The differential equations (2a) describe the synchronous machines and related primary controllers; the algebraic equations (2b) describe the classic load flow equations. See for the technical details on the power system models used the location specified in footnote 1.

Determining the evolution of the network given an initial state and input trajectory over the horizon thus requires the solution of this DAE. Solving DAEs in general is a complex task, in particular when dynamics of different time scales are present, as is the case for the power systems. Variable step size methods, e.g., DASSL [11], are suitable for these cases, since they automatically choose a larger step size

when no fast dynamics are present, and a smaller step size when they are [12]. However, using these methods inside the optimization procedure of the MPC controller could be very time-consuming and could thus result in very slow control. Therefore, such a DAE model is not directly suitable as prediction model.

Instead of taking the continuous-time DAE as prediction model, we consider a discrete-time linearized model derived from this DAE. At each discrete sampling instant  $kT_s$  the continuous-time linearization of (2a) and (2b) around  $x_0 = x(k)$ ,  $u_0 = u(k-1)$ , can be written as

$$\begin{aligned}\dot{x} &= A_c x + B_c u + F_c \\ v &= C_c x + D_c u + G_c,\end{aligned}$$

where

$$\begin{aligned}A_c &= \frac{\partial f}{\partial x} + \frac{\partial f}{\partial v} \left(-\frac{\partial g}{\partial v}\right)^{-1} \left(\frac{\partial g}{\partial x}\right), & B_c &= \frac{\partial f}{\partial u} + \frac{\partial f}{\partial v} \left(-\frac{\partial g}{\partial v}\right)^{-1} \frac{\partial g}{\partial u} \\ C_c &= \left(-\frac{\partial g}{\partial v}\right)^{-1} \frac{\partial g}{\partial x}, & D_c &= \left(-\frac{\partial g}{\partial v}\right)^{-1} \frac{\partial g}{\partial u} \\ F_c &= -\frac{\partial f}{\partial v} \left(-\frac{\partial g}{\partial v}\right)^{-1} \left(\frac{\partial g}{\partial x} x_0 + \frac{\partial g}{\partial u} u_0 + \frac{\partial g}{\partial v} v_0 - g(x_0, u_0, v_0)\right) \\ &\quad - \left(\frac{\partial f}{\partial x} x_0 + \frac{\partial f}{\partial u} u_0 + \frac{\partial f}{\partial v} v_0 - f(x_0, u_0, v_0)\right) \\ G_c &= -\left(-\frac{\partial g}{\partial v}\right)^{-1} \left(\frac{\partial g}{\partial x} x_0 + \frac{\partial g}{\partial u} u_0 + \frac{\partial g}{\partial v} v_0 - g(x_0, u_0, v_0)\right)\end{aligned}$$

when  $\frac{\partial g}{\partial v}$  is invertible, which is typically the case for power networks. The required Jacobians can either be derived analytically [13] or computed numerically. For the sake of simplicity we use the latter approach.

We assume small variations of the variables around which the model is linearized. If the variations are not small, mode changes have to be considered in the model, e.g., by using piecewise affine or similar models [13].

The continuous-time linearization is discretized with the sampling interval  $T_s$ , to obtain the following control model in the affine expressions of  $x(k)$ ,  $u(k)$  and  $v(k)$

$$\begin{aligned}x(k+1) &= Ax(k) + Bu(k) + F \\ v(k) &= Cx(k) + Du(k) + G\end{aligned}\quad (3)$$

wherein  $k$  denotes the discrete time step, and where

$$\begin{aligned}A &= e^{A_c T_s} & B &= \int_0^{T_s} e^{A_c \tau} d\tau B_c & F &= \int_0^{T_s} e^{A_c \tau} d\tau F_c \\ C &= C_c & D &= D_c & G &= G_c.\end{aligned}$$

The simulation sampling time  $T_s$  is not necessarily equal to the controller sampling time, although in the following we will take these equal. The value of  $T_s$  has to be chosen such that the discrete-time approximation adequately reflects the dynamics of the continuous-time linearized model.

The obtained discrete-time approximation is employed as a prediction model in the optimal control problem formulation. In this regard, the optimal control formulation must be augmented with the appropriate hard constraints on the inputs  $u(k) = [r(k)^T s(k)^T]^T$ , with  $r(k) = [r_1(k), \dots, r_4(k)]^T$  and  $s(k) = [s_5(k), \dots, s_9(k)]^T$ , which are physically bounded. For  $r(k)$  the admissible range is simply taken to be the continuous relaxation of the discrete physical values, since adjusting AVR set-points is not invasive. However, load shedding is more invasive and since it is an extremely

expensive control action such an approximation might not be adequate. Therefore, for  $s(k)$  the control constraints are taken as the actual discrete physically feasible values, at the cost of introducing a set of integer variables in the model; the employed control model is therefore by necessity *hybrid* in nature.

### B. Optimal control problem

To account for the control objectives mentioned in Section III with their related order of importance a cost function is formulated similarly as in [14]. To maintain the voltages  $v_1, \dots, v_9$  between 0.9 and 1.1, let the auxiliary variables  $t_j$ ,  $j = 1, \dots, 9$  defined by

$$\begin{cases} 0.9 - v_j(k) \leq t_j(k) \\ -1.1 + v_j(k) \leq t_j(k) \\ 0 \leq t_j(k) \end{cases} \quad (4)$$

denote upper bounds on the amount of violation of the voltage conditions. These upper bounds will be minimized. This formulation leads to nine variables at each sampling instant  $k$ , grouped in the vector  $t(k) = [t_1(k), \dots, t_9(k)]^T$ . To minimize the switching between control actions, define the variation of the manipulated variables as

$$\Delta u(k) = u(k) - u(k-1) = [\Delta r^T(k), \Delta s^T(k)]^T$$

and the diagonal penalty matrices

$$Q_t = \text{diag}(q_{t1}, \dots, q_{t9}), \quad Q_{\Delta u} = \text{diag}(q_{\Delta u1}, \dots, q_{\Delta u9})$$

with all penalty weights in  $\mathbb{R}^+$  and where the entries in  $Q_t$  and  $Q_{\Delta u}$  are correlated to the corresponding ordering in  $t(k)$  and  $\Delta u(k)$ . Consider now the expression for the stage cost, penalizing the worst voltage violation and input change,

$$S(k) = \|Q_t t(k)\|_\infty + \|Q_{\Delta u} \Delta u(k)\|_\infty$$

and the formulation of the cost function

$$J(x(k), u(k-1), U(k)) = \sum_{\ell=0}^{N-1} S(k+\ell|k) \quad (5)$$

which penalizes the predicted evolution  $S(k+\ell|k)$  of  $S(k)$  at step  $k+\ell$  using information available at step  $k$  over the interval  $[k, k+N]$ .

The control action at each time instant  $k$  is obtained by minimizing the objective function (5) over the sequence of control inputs  $U(k) = [u^T(k), \dots, u^T(k+N-1)]^T$  subject to the aforementioned input constraints and to inequalities (4) for the selected prediction model (3). Moreover, to reduce computational complexity, the load shedding control for the first prediction step only is computed, after which it is taken constant throughout the prediction horizon. The first step of the optimal sequence  $u^*(k)$  thus obtained is then applied to the physical network after having rounded the AVR references to the nearest feasible value. The procedure is then repeated at the successive sampling instant  $k+1$ .

Since we have a linear objective function with linear equality and inequality constraints, and since the decision variables are both continuous and discrete, the control law is the result of a mixed-integer linear programming problem,

for which there exist good commercial and free solvers (such as, e.g., CPLEX, Xpress-MP, GLPK, lp\_solve, etc. [15], [16]).

## V. SIMULATION RESULTS

### A. Scenarios

We study two scenarios. Scenario 1 starts out from the system in steady state. At 0.7 seconds the line connecting  $G_4$ , representing the largest generation capacity in the considered grid, to bus 9 changes (possibly due to a partial fault) so that its impedance increases to 150%. Fig. 3 shows the resulting open-loop evolution of the most important bus voltages. If no action is taken, voltages initially tend to progressively drift from the nominal region of operation until a series of sustained oscillations arises.

Scenario 2 involves a similar situation, only now the impedance increases to 400%, e.g., due to a forest fire. Fig. 5 shows the open-loop evolution if the higher-layer controller does not provide updated set-points to the lower-layer primary controllers. As can be seen the voltages quickly reach a series of fast oscillations.

### B. Controller setup

For our network the penalty matrices are chosen such that a weight of 200 is placed on the violation of each soft constraint; the inputs are weighted with the penalty coefficients 1 and 20 respectively for  $r(k)$  and  $s(k)$ . The prediction horizon is  $N = 8$ . At each sampling instant, the linearization point is chosen by taking the current state  $x(k)$  and the input applied at the preceding time instant  $u(k-1)$ . The sampling interval is taken to be  $T_s = 0.25$  seconds.

### C. Results

Fig. 4 depicts for scenario 1 the evolution of the system when the proposed higher-layer MPC scheme is inserted in feedback. As shown the controller prevents the voltages from exceeding the upper and lower bounds by acting on the reference settings of all the AVRs. No load shedding is necessary. The system subsequently enters an acceptable steady-state condition with a constant input profile.

Fig. 6 depicts for scenario 2 the evolution of the system with the MPC controller installed. Although the fault is significantly larger, the control prevents the voltages from crossing their limits, by providing set-points for the AVRs and shedding a minimal amount of load at node 7. After about 20 seconds the system enters a new steady-state with constant input profile.

### D. Discussion

The proposed controller works well for the studied cases, in which a rather high sampling rate of  $T_s = 0.25$  seconds was taken; indeed, this rate might have to be decreased in a more realistic setting, since the system is composed of large high-power components that may not allow for such a high actuation frequency. For the type of faults considered the simulations indicate that the predictions made with the linearized model are sufficiently accurate and that possible

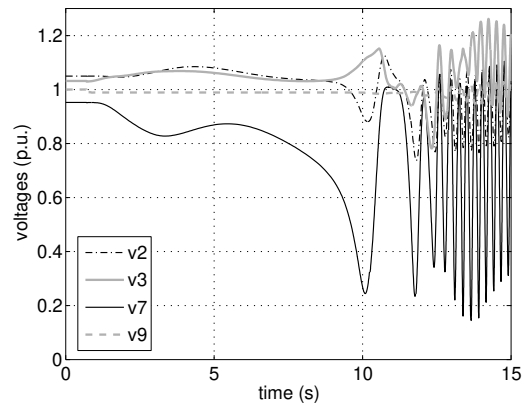
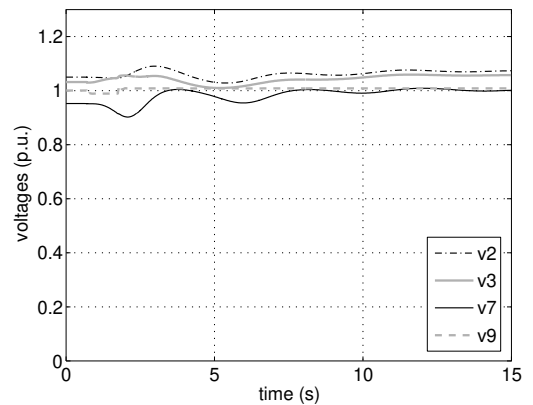
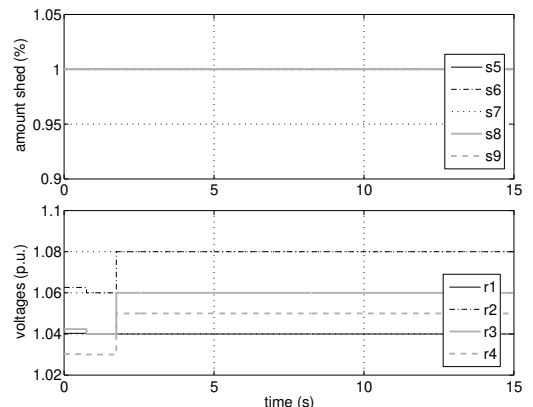


Fig. 3. Evolution of voltages in open loop for scenario 1.



(a) Evolution of voltages in closed loop.



(b) Control input sequence.

Fig. 4. Simulation results for scenario 1 in closed-loop control with the proposed MPC supervisor.

faults introduced due to saturation of the real system which are not modeled in the linearized system can be neglected. In fact, with a smaller fault, the sampling rate may be decreased, resulting in less frequent set-point updates to the lower control layer. With a smaller fault, the magnitude and frequency of oscillations occurring reduce in size.

## VI. CONCLUSIONS AND FUTURE RESEARCH

In this paper we have considered layered control of voltage instability in a particular power network. In this particular

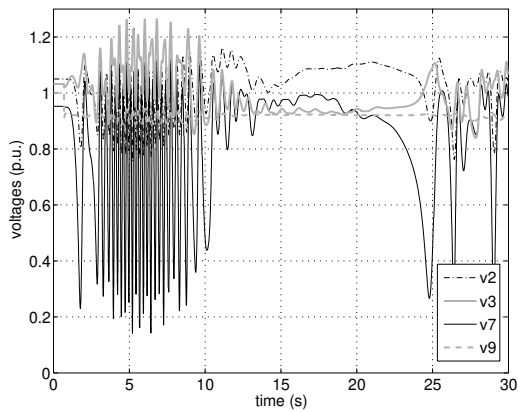
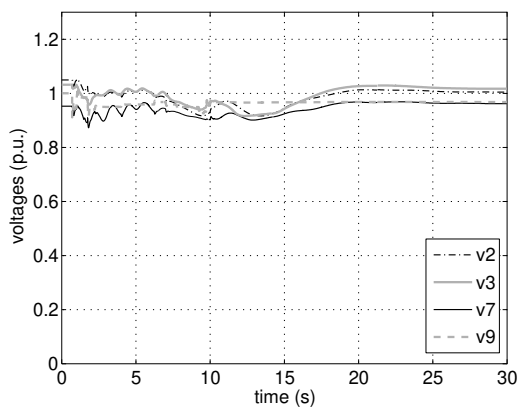
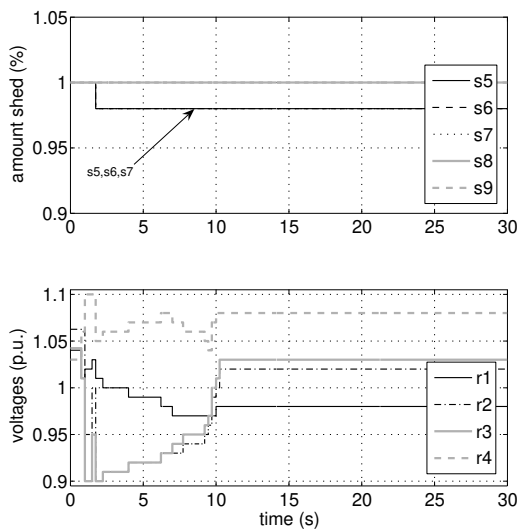


Fig. 5. Evolution of voltages in open loop for scenario 2.



(a) Evolution of voltages in closed loop.



(b) Control input sequence.

Fig. 6. Simulation results for scenario 2 in closed-loop control with the proposed MPC supervisor.

network a single higher-layer controller provides set-points to lower-layer controllers at discrete time steps such that the negative effects of voltage instabilities in the underlying physical system are minimized. The higher-layer controller uses a model predictive control strategy to determine its

actions. It uses a model based on a discrete-time linearized model of the continuous-time nonlinear dynamics given by a system of differential-algebraic equations (DAE). Simulations illustrate the potential of this supervisory approach.

Future research will focus on investigating the region of validity of the linearized model and if necessary replacing this with piecewise affine models; performing simulations on a network in which the neighboring loads and generators are not aggregated, whereas the supervisory controller uses an aggregated model; comparing the proposed approach with an approach that uses variable time steps to make the predictions, instead of the fixed time steps used currently; assessing the real-time technical viability of the method; and, investigating decentralized control schemes where the local controllers of several subnetworks negotiate among themselves on how they should determine their actions to obtain system-wide optimal performance.

#### ACKNOWLEDGMENTS

This research was supported by the project “HYbrid CONtrol: Taming Heterogeneity and Complexity of Networked Embedded Systems (HYCON)”, contract number FP6-IST-511368, the project “Multi-agent control of large-scale hybrid systems” (DWV.6188) of the Dutch Technology Foundation STW, an NWO Van Gogh grant (VGP79-99), and the BSIK project “Next Generation Infrastructures (NGI)”. We thank G. Hug-Glanzmann for her useful comments.

#### REFERENCES

- [1] U.S.-Canada Power System Outage Task Force, “Final report on the August 14, 2003 blackout in the United States and Canada: causes and recommendations,” Tech. Rep., Apr. 2004. [Online]. Available: <https://reports.energy.gov/BlackoutFinal-Web.pdf>
- [2] N. Jenkins, R. Allan, P. Crossley, D. Kirschen, and G. Strbac, *Embedded Generation*. Padstow, UK: TJ International Ltd., 2000.
- [3] J. Bernussou and A. Titli, *Interconnected Dynamical Systems: Stability, Decomposition and Decentralisation*. Amsterdam, The Netherlands: North-Holland Publishing Company, 1982.
- [4] R. G. Farmer and P. M. Anderson, *Series Compensation of Power Systems*. Encinitas, California, USA: PBLSH, Inc., 1996.
- [5] P. Kundur, *Power System Stability and Control*. New York: McGraw Hill, 1994.
- [6] D. Karlsson and D. J. Hill, “Modelling and identification of nonlinear dynamic loads in power systems,” *IEEE Transactions on Power Systems*, vol. 9, no. 1, pp. 157–163, Feb. 1994.
- [7] T. V. Cutsem and C. Vournas, *Voltage Stability of Electric Power Systems*. Dordrecht, The Netherlands: Kluwer Academic Publishers, 1998.
- [8] J. M. Maciejowski, *Predictive Control with Constraints*. Harlow, UK: Prentice Hall, 2002.
- [9] E. F. Camacho and C. Bordons, *Model Predictive Control in the Process Industry*. Berlin, Germany: Springer-Verlag, 1995.
- [10] M. Morari and J. H. Lee, “Model predictive control: past, present and future,” *Computers and Chemical Engineering*, vol. 23, pp. 667–682, 1999.
- [11] L. R. Petzold, “A description of DASSL - A differential/algebraic system solver,” in *10th World Congress on System Simulation and Scientific Computation*, Montreal, Canada, Aug. 1983, pp. 430–432.
- [12] K. E. Brenan, S. L. Campbell, and L. R. Petzold, *Numerical Solution of Initial-Value Problems in Differential-Algebraic Equations*. Philadelphia, Pennsylvania, USA: SIAM, 1996.
- [13] S. Leirens, J. Buisson, P. Bastard, and J.-L. Coullon, “A hybrid approach for voltage stability of power systems,” in *Proceedings of the 15th Power Systems Computation Conference*, Liège, Belgium, 2005.
- [14] T. Geyer, M. Larsson, and M. Morari, “Hybrid emergency voltage control in power systems,” in *Proceedings of the European Control Conference 2003*, Cambridge, UK, Sept. 2003.

- [15] A. Atamtürk and M. W. P. Savelsbergh, "Integer-programming software systems," *Annals of Operations Research*, vol. 140, no. 1, pp. 67–124, Nov. 2005.
- [16] J. Linderoth and T. Ralphs, "Noncommercial software for mixed-integer linear programming," *Optimization Online*, Jan. 2005.